NASA TECHNICAL NOTE

NASA TN D-3500

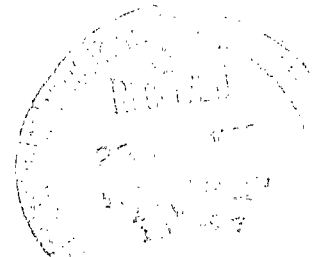c. 1

NASA TN D-3500

SUPERSONIC FLUTTER OF FLAT RECTANGULAR ORTHOTROPIC PANELS ELASTICALLY RESTRAINED AGAINST EDGE ROTATION

by Larry L. Erickson

Langley Research Center
Langley Station, Hampton, Va.

NATIONAL AERONAUTICS AND SPACE ADMINISTRATION • WASHINGTON, D.C. • AUGUST 1966

NASA TN D-3500

SUPERSONIC FLUTTER OF FLAT RECTANGULAR ORTHOTROPIC PANELS

ELASTICALLY RESTRAINED AGAINST EDGE ROTATION

By Larry L. Erickson

Langley Research Center
Langley Station, Hampton, Va.

NATIONAL AERONAUTICS AND SPACE ADMINISTRATION

SUPERSONIC FLUTTER OF FLAT RECTANGULAR ORTHOTROPIC PANELS
ELASTICALLY RESTRAINED AGAINST EDGE ROTATION

By Larry L. Erickson
Langley Research Center

SUMMARY

A theoretical solution is presented for the supersonic flutter characteristics of flat orthotropic panels subject to inplane loads and various boundary conditions. The solution is valid for panels having nondeflecting edges which are simply supported, clamped, or elastically restrained against rotation.

Numerical flutter results of the analysis are tabulated in terms of general parameters for simply supported and clamped panels and for three intermediate conditions of rotational edge restraint. From these parameters the dynamic pressure, frequency, and mode shape at flutter can be determined for large ranges of length-width ratio, stiffness ratio, and inplane stress.

INTRODUCTION

The flat rectangular panel is a basic structural element used for exterior skin surfaces of vehicles which operate within the atmosphere. The dynamic instability, or flutter, of such panels when exposed to a supersonic flow has been the subject of numerous theoretical investigations. (See ref. 1 for a summary of panel flutter research.) It has been noted in previous studies that large differences exist between the flutter boundaries of simply supported (ref. 2) and clamped (ref. 3) panels which are subjected to compressive stresses. These differences are especially prominent in the vicinity of the stress that produces buckling (ref. 4). Hence, there is a need to obtain flutter boundaries for panels whose edges are supported in a manner intermediate to the simply supported and clamped cases. To obtain these flutter boundaries, it is necessary to consider panel supports which offer resistance to edge rotation.

The flutter solutions for flat rectangular panels with various degrees of rotational edge restraint are obtained in this report. The panel edges are assumed to be restrained from angular rotations by uniform restoring moments which are of equal strength on opposite edges. There is assumed to be no displacement of the panel edges in a direction perpendicular to the plane of the panel. (Such displacements, if allowed to occur, can significantly affect the flutter boundaries as shown in ref. 5.) By accounting for the

effect of rotational edge restraint, the results presented herein should be useful in obtaining more accurate flutter boundaries of compressively stressed panels, provided that the rotational restraint of the supporting structure can be estimated.

SYMBOLS

$\overline{A}$ parameter defined by equation (6)

A_j constants appearing in equation (11);   j = 1, 2, 3, 4

a   panel length in x-direction

$\overline{B}$ parameter defined by equation (6)

$B_1, B_2, B_3, B_4, B_5, B_6$ coefficients defined by equation (A3)

b   panel width in y-direction

C_0, C_1, C_2 coefficients defined by equation (9)

D_x, D_y panel bending stiffness in x-direction and y-direction, respectively

D_{xy} panel twisting stiffness

D_1, D_{12}, D_2 panel stiffness coefficients defined by equation (8)

F   expression for the determinant appearing in equation (17)

j,k   integers

k_x nondimensional stress coefficient, $\dfrac{N_x b^2}{\pi^2 D_1}$

k_y nondimensional stress coefficient, $\dfrac{N_y b^2}{\pi^2 D_1}$

l aerodynamic pressure load per unit area given by equation (2)

M   Mach number

m_j roots of equation (12);   j = 1, 2, 3, 4

2

N_x inplane loading in x-direction, positive in compression

N_y inplane loading in y-direction, positive in compression

q dynamic pressure of airflow, $\frac{1}{2}\rho_a V^2$

q_x rotational restraint coefficient on leading- and trailing-edge boundaries, $\dfrac{a\theta_x}{D_1}$

q_y rotational restraint coefficient on side-edge boundaries, $\dfrac{b\theta_y}{D_2}$

S_1, S_2, S_3 coefficients defined by equation (16)

t time

V velocity of airflow

w lateral deflection of panel

X, Y functions of x only and y only, respectively, used in approximate solution to equation (1)

x, y, z rectangular Cartesian coordinates (see fig. 1)

α, δ, ϵ components of the roots m_j (see eq. (13))

$\beta = \sqrt{M^2 - 1}$

$\bar{\epsilon} = i\epsilon$

θ_x spring constant of rotational springs supporting panel at $x = 0$ and $x = a$

θ_y spring constant of rotational springs supporting panel at $y = 0$ and $y = b$

λ dynamic pressure parameter, $\dfrac{2qa^3}{\beta D_1}$

μ_x, μ_y Poisson's ratio in x- and y-directions, respectively

ρ_a mass density of airflow

3

ρ_m mass density of panel per unit area

ω panel frequency

ω_0 reference frequency, $\sqrt{\dfrac{\pi^4 D_1}{b^4 \rho_m}}$

Subscripts:

cr   denotes critical or flutter value

T   denotes transition value (where frequency becomes zero and panel is on verge of buckling)

ANALYSIS

The configuration analyzed consists of a flat rectangular orthotropic panel which is of length a and width b as shown in figure 1. The panel is subjected to uniform inplane force intensities N_x and N_y which are considered positive in compression. The inplane shear intensity is taken to be zero. The panel is supported in such a manner that there is no lateral deflection along the edges. In addition, the edges are elastically restrained against rotation by a uniform restoring moment which is proportional to the slope of the panel at the boundaries. The proportionality between restoring moment and slope is assumed to be equal on opposite edges. The supersonic flow at Mach number M is over the top surface of the panel and is parallel to the X-axis.

Differential Equation and Boundary Conditions

The differential equation governing the lateral vibrations of a flat orthotropic panel is obtained from reference 6 by neglecting terms involving shear deformations and by adding a transverse inertia term

$$\frac{D_x}{1 - \mu_x \mu_y} \frac{\partial^4 w}{\partial x^4} + 2\left(D_{xy} + \frac{\mu_y D_x}{1 - \mu_x \mu_y}\right) \frac{\partial^4 w}{\partial x^2 \partial y^2} + \frac{D_y}{1 - \mu_x \mu_y} \frac{\partial^4 w}{\partial y^4}$$

$$+ N_x \frac{\partial^2 w}{\partial x^2} + N_y \frac{\partial^2 w}{\partial y^2} + \rho_m \frac{\partial^2 w}{\partial t^2} = l \tag{1}$$

In this equation, D_x and D_y are the panel bending stiffnesses in the x- and y-directions, respectively; D_{xy} is the panel twisting stiffness; μ_x and μ_y are Poisson's ratios in the x- and y-directions, respectively; ρ_m is the mass density per

4

unit area of the panel and l is the lateral pressure due to the airflow. The aerodynamic loading is assumed to be given by two-dimensional static aerodynamics so that

$$l = \frac{-2q}{\beta} \frac{\partial w}{\partial x} \qquad (2)$$

where $q = \frac{1}{2}\rho_a V^2$ is the dynamic pressure and $\beta = \sqrt{M^2 - 1}$. Reference 7 has shown that for Mach numbers greater than about 1.5, the use of this simple expression to represent the aerodynamic pressure load leads, in most cases, to the same flutter results as the use of more exact aerodynamics.

The boundary conditions which the solution to equation (1) must satisfy are

$$\left. \begin{aligned} \frac{D_x}{1 - \mu_x \mu_y} \frac{\partial^2 w}{\partial x^2} - \theta_x \frac{\partial w}{\partial x} = 0 \quad \text{and} \quad w = 0 \quad \text{at} \quad x = 0 \\[2mm] \frac{D_x}{1 - \mu_x \mu_y} \frac{\partial^2 w}{\partial x^2} + \theta_x \frac{\partial w}{\partial x} = 0 \quad \text{and} \quad w = 0 \quad \text{at} \quad x = a \end{aligned} \right\} \qquad (3a)$$

$$\left. \begin{aligned} \frac{D_y}{1 - \mu_x \mu_y} \frac{\partial^2 w}{\partial y^2} - \theta_y \frac{\partial w}{\partial y} = 0 \quad \text{and} \quad w = 0 \quad \text{at} \quad y = 0 \\[2mm] \frac{D_y}{1 - \mu_x \mu_y} \frac{\partial^2 w}{\partial y^2} + \theta_y \frac{\partial w}{\partial y} = 0 \quad \text{and} \quad w = 0 \quad \text{at} \quad y = b \end{aligned} \right\} \qquad (3b)$$

where θ_x and θ_y are the spring constants (per unit length) of the rotational restraints acting at the boundaries.

Solution of Differential Equation

In general, a product solution of the form

$$w(x,y,t) = X\left(\frac{x}{a}\right) Y\left(\frac{y}{b}\right) e^{i\omega t} \qquad (4)$$

where ω is the panel frequency, will not satisfy equation (1) since the term $\dfrac{\partial^4 w}{\partial x^2 \partial y^2}$ prevents the functions X and Y from separating. However, an approximate solution in the form of equation (4) can be obtained by use of a method given by Kantorovich (ref. 8). If $Y(y/b)$ is assumed to be some function (as yet unspecified) which satisfies the boundary conditions given by equations (3b), then equation (1) can be reduced to an ordinary differential equation by the following procedure:

5

(1) In equation (1), $w(x,y,t)$ and l are replaced with equations (4) and (2), respectively.

(2) The resulting equation is multiplied by $Y(y/b)$ and integrated with respect to y/b.

This procedure yields

$$X''''\left(\frac{x}{a}\right) + \pi^2 \overline{A} X''\left(\frac{x}{a}\right) + \lambda X'\left(\frac{x}{a}\right) - \pi^4 \overline{B} X\left(\frac{x}{a}\right) = 0 \tag{5}$$

where a prime indicates differentiation with respect to x/a and

$$\overline{A} = \left(\frac{a}{b}\right)^2 \left[k_x + 2\left(\frac{D_{12}}{D_1}\right)\left(\frac{1}{\pi^2}\frac{C_1}{C_0}\right)\right] \tag{6a}$$

$$\lambda = \frac{2qa^3}{\beta D_1} \tag{6b}$$

$$\overline{B} = \left(\frac{a}{b}\right)^4 \left[\left(\frac{\omega}{\omega_0}\right)^2 - k_y\left(\frac{1}{\pi^2}\frac{C_1}{C_0}\right) - \left(\frac{D_2}{D_1}\right)\left(\frac{1}{\pi^4}\frac{C_2}{C_0}\right)\right] \tag{6c}$$

$$\left.\begin{aligned}
k_x &= \frac{N_x b^2}{\pi^2 D_1} \\[2mm]
k_y &= \frac{N_y b^2}{\pi^2 D_1} \\[2mm]
\omega_0{}^2 &= \frac{\pi^4 D_1}{\rho_m b^4}
\end{aligned}\right\} \tag{7}$$

$$\left.\begin{aligned}
D_1 &= \frac{D_x}{1 - \mu_x \mu_y} \\[3mm]
D_{12} &= D_{xy} + \frac{\mu_y D_x}{1 - \mu_x \mu_y} \\[3mm]
D_2 &= \frac{D_y}{1 - \mu_x \mu_y}
\end{aligned}\right\} \tag{8}$$

The coefficients C_0, C_1, and C_2 are due to the integrals involving $Y(y/b)$ and are given by

6

$$C_0 = \int_0^1 Y^2\left(\frac{y}{b}\right)d\left(\frac{y}{b}\right)$$

$$C_1 = \int_0^1 Y\left(\frac{y}{b}\right)Y''\left(\frac{y}{b}\right)d\left(\frac{y}{b}\right) \qquad (9)$$

$$C_2 = \int_0^1 Y\left(\frac{y}{b}\right)Y''''\left(\frac{y}{b}\right)d\left(\frac{y}{b}\right)$$

where a prime indicates differentiation with respect to y/b.

Thus, by selection of an appropriate function for $Y(y/b)$, the problem is reduced to finding the exact solution of equation (5) which satisfies the following boundary conditions:

$$X(0) = X(1) = 0$$

$$X''(0) - q_x X'(0) = 0 \qquad (10)$$

$$X''(1) + q_x X'(1) = 0$$

where

$$q_x = \frac{a\theta_x}{D_1}$$

is defined as the rotational restraint coefficient.

The general solution to equation (5) is

$$X\left(\frac{x}{a}\right) = A_1 e^{m_1\frac{x}{a}} + A_2 e^{m_2\frac{x}{a}} + A_3 e^{m_3\frac{x}{a}} + A_4 e^{m_4\frac{x}{a}} \qquad (11)$$

where m_j (j = 1, 2, 3, 4) satisfies the auxiliary equation

$$m^4 + \pi^2 \overline{A} m^2 + \lambda m - \pi^4 \overline{B} = 0 \qquad (12)$$

Equation (12) is of the same form as that solved by Hedgepeth (ref. 2) who assumed that the roots are

$$m_1 = \alpha + i\delta$$

$$m_2 = \alpha - i\delta$$

$$m_3 = -\alpha + \epsilon \qquad (13)$$

$$m_4 = -\alpha - \epsilon$$

From the relations between the sum of the roots (taken one, two, three, and four at a time) and the coefficients of a polynomial equation, the following expressions are obtained:

$$\delta^2 = \frac{\lambda}{4\alpha} + \alpha^2 + \pi^2 \frac{\overline{A}}{2} \tag{14a}$$

$$\epsilon^2 = \frac{\lambda}{4\alpha} - \alpha^2 - \pi^2 \frac{\overline{A}}{2} \tag{14b}$$

$$\pi^4 \overline{B} = \left(\frac{\lambda}{4\alpha}\right)^2 - 4\left(\alpha^2 + \frac{\pi^2 \overline{A}}{4}\right)^2 \tag{14c}$$

Equation (14c) can be written as

$$\alpha^6 + S_1 \alpha^4 + S_2 \alpha^2 - S_3 = 0 \tag{15}$$

where

$$\left.\begin{aligned} S_1 &= \pi^2 \frac{\overline{A}}{2} \\ S_2 &= \frac{1}{4}\left[\pi^4 \overline{B} + \left(\frac{\pi^2 \overline{A}}{2}\right)^2\right] \\ S_3 &= \left(\frac{\lambda}{8}\right)^2 \end{aligned}\right\} \tag{16}$$

Thus, α can be determined from equation (15) for given values of the coefficients $\overline{A}$, λ, and $\overline{B}$. The solution to equation (12) is then readily determined since δ and ϵ can now be calculated and hence the roots m_j are known.

Satisfaction of Boundary Conditions at the Leading and Trailing Edges

Application of the boundary conditions, given by equations (10), to equation (11) gives

$$\begin{bmatrix} 1 & 1 & 1 & 1 \\ m_1(m_1 - q_x) & m_2(m_2 - q_x) & m_3(m_3 - q_x) & m_4(m_4 - q_x) \\ e^{m_1} & e^{m_2} & e^{m_3} & e^{m_4} \\ m_1(m_1 + q_x)e^{m_1} & m_2(m_2 + q_x)e^{m_2} & m_3(m_3 + q_x)e^{m_3} & m_4(m_4 + q_x)e^{m_4} \end{bmatrix} \begin{Bmatrix} A_1 \\ A_2 \\ A_3 \\ A_4 \end{Bmatrix} = \begin{Bmatrix} 0 \\ 0 \\ 0 \\ 0 \end{Bmatrix} \tag{17}$$

The condition for a nontrivial solution is obtained by equating the determinant of the square matrix to zero. This yields

$$F\left(m_1, m_2, m_3, m_4\right) = \left(m_4{}^2 - m_3{}^2\right)\left(m_2{}^2 - m_1{}^2\right)\left(e^{m_3+m_4} + e^{m_1+m_2}\right)$$

$$+ \left(m_4{}^2 - m_2{}^2\right)\left(m_1{}^2 - m_3{}^2\right)\left(e^{m_2+m_4} + e^{m_1+m_3}\right)$$

$$+ \left(m_4{}^2 - m_1{}^2\right)\left(m_3{}^2 - m_2{}^2\right)\left(e^{m_1+m_4} + e^{m_2+m_3}\right)$$

$$+ q_x\left(m_2 - m_1\right)\left(m_4 - m_3\right)\left[\left(m_1 + m_2\right) - \left(m_3 + m_4\right)\right]\left(e^{m_3+m_4} - e^{m_1+m_2}\right)$$

$$+ q_x\left(m_1 - m_3\right)\left(m_4 - m_2\right)\left[\left(m_1 - m_2\right) + \left(m_3 - m_4\right)\right]\left(e^{m_2+m_4} - e^{m_1+m_3}\right)$$

$$+ q_x\left(m_4 - m_1\right)\left(m_3 - m_2\right)\left[\left(m_2 - m_1\right) + \left(m_3 - m_4\right)\right]\left(e^{m_1+m_4} - e^{m_2+m_3}\right)$$

$$- q_x{}^2\left(m_4 - m_3\right)\left(m_2 - m_1\right)\left(e^{m_3+m_4} + e^{m_1+m_2}\right)$$

$$- q_x{}^2\left(m_4 - m_2\right)\left(m_1 - m_3\right)\left(e^{m_2+m_4} + e^{m_1+m_3}\right)$$

$$- q_x{}^2\left(m_4 - m_1\right)\left(m_3 - m_2\right)\left(e^{m_1+m_4} + e^{m_2+m_3}\right) = 0 \tag{18}$$

Replacement of the roots m_j with the expressions given by equations (13) yields

$$F(\alpha, \delta, \epsilon) = \left[\left(\epsilon^2 + \delta^2\right)^2 - 4\alpha^2\left(\epsilon^2 - \delta^2\right)\right]\sinh \epsilon \ \sin \delta - 8\alpha^2\epsilon \delta(\cosh \epsilon \ \cos \delta - \cosh 2\alpha)$$

$$+ 2q_x\left[4\alpha\delta\epsilon \ \sinh 2\alpha + \epsilon\left(\epsilon^2 + \delta^2 - 4\alpha^2\right)\cosh \epsilon \ \sin \delta - \delta\left(\epsilon^2 + \delta^2 + 4\alpha^2\right)\sinh \epsilon \ \cos \delta\right]$$

$$+ q_x{}^2\left[2\epsilon \delta(\cosh 2\alpha - \cosh \epsilon \ \cos \delta) + \left(\epsilon^2 - \delta^2 - 4\alpha^2\right)\sinh \epsilon \ \sin \delta\right] = 0 \tag{19}$$

For the case where the panel is simply supported at $x = (0, a)$, q_x equals zero and equation (19) reduces to the solution obtained by Hedgepeth (ref. 2). For the case where the panel is clamped at $x = (0, a)$, q_x is infinite and equation (19) reduces to the solution obtained by Houbolt (ref. 3).

Numerical calculations show that for values of $\overline{A}$ greater than about 4, equation (14b) yields $\epsilon^2 < 0$. When this situation occurs it is convenient to define $\overline{\epsilon} = \sqrt{-\epsilon^2} = i\epsilon$ so that equation (19) becomes

$$F(\alpha, \delta, \overline{\epsilon}) = \left[\left(\delta^2 - \overline{\epsilon}^2\right)^2 + 4\alpha^2\left(\delta^2 + \epsilon^2\right)\right]\sin \overline{\epsilon} \sin \delta - 8\alpha^2\overline{\epsilon}\delta(\cos \overline{\epsilon} \cos \delta - \cosh 2\alpha)$$

$$+ 2q_x\left[4\alpha\overline{\epsilon}\delta \sinh 2\alpha + \overline{\epsilon}\left(\delta^2 - \overline{\epsilon}^2 - 4\alpha^2\right)\cos \overline{\epsilon} \sin \delta - \delta\left(\delta^2 - \overline{\epsilon}^2 + 4\alpha^2\right)\sin \overline{\epsilon} \cos \delta\right]$$

$$+ q_x^2\left[2\overline{\epsilon}\delta(\cosh 2\alpha - \cos \overline{\epsilon} \cos \delta) - \left(\delta^2 + \overline{\epsilon}^2 + 4\alpha^2\right)\sin \overline{\epsilon} \sin \delta\right] = 0 \qquad (20)$$

The derivation of the panel mode shape associated with equation (19) is presented in the appendix along with a discussion of the modal characteristics.

Flutter Condition and Procedure for Obtaining Numerical Results

Equation (19) or (20) implicitly gives the panel frequency parameter $\overline{B}$ in terms of the dynamic pressure parameter λ. When λ reaches a certain critical value, designated λ_{cr}, two of the panel frequencies coalesce. An increase in λ above λ_{cr} causes $\overline{B}$, and hence ω^2, to become complex. Thus, one of the two square roots of ω^2 must possess a negative imaginary part which by equation (4) produces a divergent motion, termed flutter. The point where two frequencies coalesce is characterized by the condition $\partial\lambda/\partial\overline{B} = 0$ (see ref. 2) and corresponds to the values of λ_{cr} and $\overline{B}_{cr}$ presented in this report.

For given values of the rotational restraint coefficient q_x and the parameter $\overline{A}$, the following procedure was used to calculate the numerical flutter solutions presented herein:

(1) A reasonable value was chosen for the parameter $\overline{B}$ and a trial value of λ was selected.

(2) The quantity α was calculated from equation (15).

(3) The quantities δ and ϵ were then determined from equations (14a) and (14b).

(4) Equation (19) or (20) was used to calculate $F(\alpha, \delta, \epsilon)$; a nonzero value indicated an incorrect choice of λ. (From a programing aspect, it is more convenient to calculate $F(\alpha, \delta, \epsilon)$ from eq. (18), provided that a digital computer capable of working in complex arithmetic is available.)

(5) The procedure was repeated with different values of λ until the transcendental equation $F(\alpha, \delta, \epsilon) = 0$ was satisfied within a 0.01-percent error in λ, thus giving a point on a λ-$\overline{B}$ plot.

By repeating the process for additional choices of $\overline{B}$, the frequency loop (variation in λ with $\overline{B}$) was obtained for the given values of q_x and $\overline{A}$. The quantities λ_{cr} and

$\overline{B}_{cr}$ were then determined from the point on the frequency loop where $\partial\lambda/\partial\overline{B} = 0$. A typical plot showing the first two frequency loops for the simply supported and clamped cases is shown in figure 2.

<center>Preflutter Solution</center>

When large negative values of the parameter $\overline{A}$ are considered, the exact solution for λ_{cr} becomes difficult to determine numerically. However, as discussed in the next section, it is in this range of $\overline{A}$ that a simple algebraic solution can be used to obtain good approximations to both λ_{cr} and $\overline{B}_{cr}$. The algebraic solution is obtained by noting that for either simply supported $(q_x = 0)$ or clamped $(q_x = \infty)$ panels, equation (19) is identically satisfied if $\delta = 2k\pi$ and $\epsilon = 2\alpha$, where k is an integer. This solution was first noticed by Movchan (ref. 9). With the use of these expressions for δ and ϵ, equations (14) yield the following simple algebraic solution for λ and $\overline{B}$ which has been denoted as the preflutter solution

$$\left.\begin{aligned} \lambda &= \frac{4}{3}\pi^3\left(10k^2 - \overline{A}\right)\sqrt{\frac{4k^2 - \overline{A}}{6}} \\ \overline{B} &= \frac{4}{3}k^2\left(7k^2 - 2\overline{A}\right) + \frac{\overline{A}^2}{12} \end{aligned}\right\} \tag{21}$$

For a given value of $\overline{A}$, these two expressions determine the points where the frequency loops of the simply supported panel intersect those of the clamped panel. As shown in figure 2 the integer k indicates the loops which intersect. The lowest value of λ is obtained by setting $k = 1$; thus, the preflutter equation for λ with $k = 1$ always yields $\lambda \leq \lambda_{cr}$. Note that with $k = 1$, the preflutter solution is valid only for $\overline{A} \leq 4$.

<center>RESULTS AND DISCUSSION</center>

The primary results of the analysis are presented in table I for $q_x = 0, 2, 10, 40,$ and ∞. For each value of q_x the values of λ_{cr} and $\overline{B}_{cr}$ are tabulated for a wide range of the parameter $\overline{A}$. The corresponding values of α_{cr} are also given in table I so that mode shapes can be calculated from equation (A2). The variation of λ_{cr} and $\overline{B}_{cr}$ with $\overline{A}$ is presented in figures 3 and 4, respectively, for $\overline{A} \leq -1$. For $\overline{A} \geq -1$, the variation of λ_{cr} with $\overline{A}$ is presented in figures 5, 6, 7, 8, and 9 for $q_x = 0, 2, 10, 40,$ and ∞, respectively.

In figure 3 the parameter $\lambda_{cr}^{1/3}/\sqrt{-\overline{A}}$, which does not contain the panel length a, is plotted against negative values of $\overline{A}$ for various values of q_x. As $-\overline{A}$ becomes large (implying large length-width ratios if the inplane load N_x is zero) the results become nearly constant. Because the parameter $\lambda_{cr}^{1/3}/\sqrt{-\overline{A}}$ does not contain the panel length a, this behavior indicates that the flutter dynamic pressure has become independent of the panel length. At a value of $\overline{A}$ near -100 the clamped $(q_x = \infty)$ and the simply supported $(q_x = 0)$ flutter boundaries have merged. Consequently, for $\overline{A} \leq -100$, the amount of rotational restraint acting at the leading and trailing edges no longer has an effect on λ_{cr}. At a value of $\overline{A}$ near -300 the exact flutter boundary (for $0 \leq q_x \leq \infty$) has merged with the preflutter solution (k = 1). Thus, regardless of the amount of rotational edge restraint acting at the leading and trailing edges, λ_{cr} can be obtained from the preflutter solution (eq. (21)) for any panel configuration having an $\overline{A} \leq -300$. Note that, for $q_x = 0$, the preflutter solution is quite accurate for any negative $\overline{A}$.

In figure 4 the parameter $\overline{B}_{cr}/(-\overline{A})^2$ (which also does not contain the panel length a) is plotted against negative values of $\overline{A}$. This parameter also becomes constant as $-\overline{A}$ becomes large. Hence, for stress-free panels with large length-width ratios, the flutter frequency is independent of the panel length.

Compressively Stressed Panels

For panels which are subjected to compressive inplane force intensities in the flow direction, $\overline{A}$ can take on positive values. The flutter boundaries in this case are shown in figures 5 to 9 as plots of $\lambda_{cr}^{1/3}$ against $\overline{A}$ for values of $\overline{A}$ from -1 to 21. (The cube root of the flutter parameter is introduced merely for convenience in plotting.) Two boundaries are shown in each of these figures. The solid boundary results from the coalescence of the lowest two natural frequencies. The dashed boundary is obtained from the coalescence of the next two higher frequencies. For any value of $\overline{A}$, the flutter value of λ is determined by the curve that gives the smaller value of the ordinate. The preflutter solution (with k = 1) is included in figure 5 for comparison with the exact flutter boundary of a simply supported panel $(q_x = 0)$. The results show that the preflutter solution gives a reasonably good approximation to λ_{cr} for a panel with simply supported leading and trailing edges whenever $\overline{A} \leq 3$.

The flutter boundaries in figures 5 to 9 indicate that the degree of rotational edge restraint can greatly affect the flutter behavior of compressively stressed panels. This influence of boundary conditions can be more clearly seen in figure 10 where $\lambda_{cr}^{1/3}$ is plotted against the midplane stress ratio k_x/k_{xT} for a particular panel configuration and for several values of the rotational restraint coefficient q_x. The panel is isotropic $(D_1 = D_{12} = D_2)$ with a/b = 3, $N_y/N_x = 1$, and $\theta_x/\theta_y = 1$. The boundaries

shown were constructed from the numerical values of λ_{cr} and $\overline{B}_{cr}$ presented in table I. The quantity k_{xT} is the transition value of k_x; that is, that value of k_x which produces buckling ($\omega = 0$). Such a plot is often used in correlating experimental results when the ratio of the applied stress to the buckling stress can be estimated even though the magnitude of the stress is unknown. Experiments indicate that the transition point $\left(k_x = k_{xT}\right)$ is the lowest point on the flutter boundary since a further increase in stress (panel buckled) usually has a stabilizing influence (ref. 4, fig. 14). For $k_x = 0$, the edge support conditions affect the panel behavior in an expected way; that is, an increase in rotational restraint q_x is accompanied by an increase in λ_{cr}. However, as k_x/k_{xT} increases, this behavior is completely reversed. For instance, when fixed values of k_x/k_{xT} are greater than about 0.4 the effect of stiffening the panel supports is to lower the dynamic pressure required to induce flutter. Further increases in k_x/k_{xT} result in a wide divergence of the boundaries. It should be noted however that the abscissa of figure 10 represents the inplane load as a percentage of the buckling load. This buckling load k_{xT} varies with q_x as shown. Hence, for a given value of $k_x/k_{xT} \neq 0$, each panel configuration shown $\left(q_x = 0, 10, \infty\right)$ carries a different inplane load.

For a given panel configuration, the variation of flutter frequency with stress is given in figure 11 where $\overline{B}_{cr}$ is plotted against positive $\overline{A}$ for simply supported panels (fig. 11(a)) and clamped panels (fig. 11(b)). The solid lines correspond to the flutter frequencies associated with the solid flutter boundaries shown in figures 5 and 9. Superimposed on figures 11(a) and 11(b) are dashed lines which indicate panel natural frequencies (i.e., $\lambda = 0$). For the range of $\overline{A}$ shown, the flutter frequencies lie between the two lowest natural frequencies. Note, however, that the two lowest frequencies do not always correspond to the first and second mode shapes. (See ref. 10 for a detailed discussion of this behavior.) Values of $\overline{B}_{cr}$ for other values of q_x can be obtained from table I; the curves shown in figures 11(a) and 11(b) are typical of the results for all values of q_x.

The theoretical results presented herein show that flutter is possible at zero dynamic pressure. It has been shown in reference 11 that, if damping is considered, flutter at zero dynamic pressure does not occur. However, the resulting theoretical flutter boundaries, which include the effect of damping, still do not agree well with experimental boundaries (ref. 7). The theoretical effect of damping then would be to smooth out, but not eliminate, the saw-tooth nature of the flutter boundaries in figures 5 to 9. Thus, these flutter boundaries should not be considered reliable in the regions of positive $\overline{A}$ for which the theoretical values of λ_{cr} are near zero.

Application of Results

The results of the analysis show λ_{cr} to be a function only of $\overline{A}$ and the rotational restraint at the leading and trailing edges. The effect of the rotational restraint along the streamwise edges on the flutter solution is reflected in the coefficients C_1/C_0 and C_2/C_0 which appear in $\overline{A}$ and $\overline{B}$. Before the results tabulated in table I can be applied to a specific configuration, these coefficients must be determined. Values of these coefficients were obtained in reference 10 by the use of beam modes for the mode shape $Y(y/b)$ appearing in equations (9). The beam modes considered satisfy the boundary conditions (3b). Thus, the resulting values of C_1/C_0 and C_2/C_0 are functions of the rotational edge restraint θ_y along the boundaries parallel to the flow. The results for the first symmetrical mode are taken from reference 10 and presented in figures 12 and 13 where the variations in C_1/C_0 and C_2/C_0, respectively, with $q_y = \dfrac{b\theta_y}{D_2}$ are shown. Only the solution for the first mode is shown here since it usually yields the most critical flutter condition. (Ref. 10 presents solutions for the first four modes.)

Once the ratio C_1/C_0 is known, the parameter $\overline{A}$ can be determined from equation (6a) for a given panel configuration and stress condition. Then, for a specified amount of rotational edge restraint along the boundaries perpendicular to the flow (given by q_x), the flutter value of λ and $\overline{B}$ can be determined from table I or from the figures showing λ_{cr} and $\overline{B}_{cr}$ as a function of $\overline{A}$ and q_x. The flutter frequency can then be determined from equation (6c). It is important to make this calculation for the frequency because a nonpositive value of $\left(\omega/\omega_0\right)^2$ indicates that the panel is buckled, and the flutter boundaries presented herein are no longer valid.

Throughout this section it has been implied that the spring constants θ_x and θ_y are known. These constants will, of course, depend on the configuration of the structure which supports the panel. The values can be obtained either from a stiffness analysis of the supporting structure or from experimental vibration frequencies of the supported panels.

It should be remembered that the solutions presented herein are approximate unless the side edges $(y = 0,b)$ are simply supported, in which case they are exact. However, the vibration and buckling results of reference 10, which were obtained by using the same approximation as used herein, were in good agreement with exact solutions. Therefore, except in cases where consideration of damping and exact aerodynamics is important, the flutter results presented in this report are expected to be reasonably accurate.

CONCLUSIONS

The theoretical solution is obtained for the flutter behavior of a flat orthotropic rectangular panel supported in such a manner that the rotations of the panel edges are elastically restrained. The solution is in terms of general parameters which account for dynamic pressure, Mach number, panel frequency, length-width ratio, inplane stress, panel stiffnesses, and edge support conditions. Numerical flutter values of these parameters are tabulated for simply supported and clamped panels and for three intermediate conditions of rotational edge restraint. From the results of the analysis, the following conclusions can be drawn:

1. The flutter boundary for compressively stressed panels is very sensitive to the panel support conditions.

2. When the length-width ratio is large the flutter dynamic pressure and frequency for stress-free panels are insensitive to the support conditions at the leading and trailing edges and the panel length.

3. The simple algebraic preflutter expression can be used to calculate the flutter boundary for a wide range of parameters with good accuracy.

Langley Research Center,
    National Aeronautics and Space Administration,
        Langley Station, Hampton, Va., February 23, 1966.

APPENDIX

MODAL BEHAVIOR

The panel mode shape can be obtained from equation (11) once the coefficients A_j are known. These coefficients can be obtained, within an arbitrary constant C, from equation (17)

$$
\left.
\begin{aligned}
A_1 &= C \begin{vmatrix} 1 & 1 & 1 \\ m_2(m_2 - q_x) & m_3(m_3 - q_x) & m_4(m_4 - q_x) \\ e^{m_2} & e^{m_3} & e^{m_4} \end{vmatrix} \\[2ex]
A_2 &= -C \begin{vmatrix} 1 & 1 & 1 \\ m_1(m_1 - q_x) & m_3(m_3 - q_x) & m_4(m_4 - q_x) \\ e^{m_1} & e^{m_3} & e^{m_4} \end{vmatrix} \\[2ex]
A_3 &= C \begin{vmatrix} 1 & 1 & 1 \\ m_1(m_1 - q_x) & m_2(m_2 - q_x) & m_4(m_4 - q_x) \\ e^{m_1} & e^{m_2} & e^{m_4} \end{vmatrix} \\[2ex]
A_4 &= -C \begin{vmatrix} 1 & 1 & 1 \\ m_1(m_1 - q_x) & m_2(m_2 - q_x) & m_3(m_3 - q_x) \\ e^{m_1} & e^{m_2} & e^{m_3} \end{vmatrix}
\end{aligned}
\right\}
\tag{A1}
$$

Substitution of these expressions for A_j into equation (11) and replacing the m_j with the expressions given by equations (13) yields, after considerable manipulation,

$$
\frac{X\left(\frac{x}{a}\right)}{4iC} = \left(B_1 + q_x B_4\right) e^{\alpha\frac{x}{a}} \sin \delta \frac{x}{a} + \left(B_2 + q_x B_5\right)\left(e^{-\alpha\frac{x}{a}} \cosh \epsilon \frac{x}{a} - e^{\alpha\frac{x}{a}} \cos \delta \frac{x}{a}\right)
$$

$$
+ \left(B_3 + q_x B_6\right) e^{-\alpha\frac{x}{a}} \sinh \epsilon \frac{x}{a}
\tag{A2}
$$

where

$$B_1 = 2\alpha\epsilon\left(e^{\alpha}\cos\delta - e^{-\alpha}\cosh\epsilon\right) - \left(\epsilon^2 + \delta^2\right)e^{-\alpha}\sinh\epsilon$$

$$B_2 = 2\alpha\epsilon\,e^{\alpha}\sin\delta + 2\alpha\delta e^{-\alpha}\sinh\epsilon$$

$$B_3 = \left(\epsilon^2 + \delta^2\right)e^{\alpha}\sin\delta + 2\alpha\delta\left(e^{\alpha}\cos\delta - e^{-\alpha}\cosh\epsilon\right)$$

$$B_4 = \epsilon\left(e^{\alpha}\cos\delta - e^{-\alpha}\cosh\epsilon\right) - 2\alpha e^{-\alpha}\sinh\epsilon$$

$$B_5 = \epsilon\,e^{\alpha}\sin\delta - \delta e^{-\alpha}\sinh\epsilon$$

$$B_6 = 2\alpha e^{\alpha}\sin\delta - \delta\left(e^{\alpha}\cos\delta - e^{-\alpha}\cosh\epsilon\right)$$

(A3)

Equation (A2) satisfies the first three boundary conditions (eqs. (10)) identically and satisfies the fourth only if the transcendental equation $F(\alpha,\delta,\epsilon) = 0$ is satisfied.

The theoretical mode shape at flutter is strongly influenced by compressive values of the loading N_x. This effect is indicated by the following table which shows the number of nodes and the region where the maximum amplitude occurs for simply supported and clamped panels. (Increasing $\overline{A}$ reflects increasing compressive values of N_x.)

$\overline{A}$	Maximum amplitude occurs toward –		Number of nodes	
	Simply supported	Clamped	Simply supported	Clamped
-10	Trailing edge	Trailing edge	1	1
0	Trailing edge	Trailing edge	1	1
3	Trailing edge	Trailing edge	1	1
6	Leading edge	Trailing edge	1	1
9	Leading edge	Trailing edge	1	2
12	Trailing edge	Leading edge	2	1

Correlation of the information presented in this table with figures 11(a) and 11(b) shows that the point of maximum amplitude moves from the rear of the panel to the front and back again as $\overline{A}$ passes the points where natural frequency lines cross. The flutter mode shapes at $\overline{A} = 12$ are shown in figure 14 for three different values of q_x.

REFERENCES

1. Fung, Y. C.: Some Recent Contributions to Panel Flutter Research. AIAA J., vol. 1, no. 4, Apr. 1963, pp. 898-909.

2. Hedgepeth, John M.: Flutter of Rectangular Simply Supported Panels at High Supersonic Speeds. J. Aeron. Sci., vol. 24, no. 8, Aug. 1957, pp. 563-573, 586.

3. Houbolt, John C.: A Study of Several Aerothermoelastic Problems of Aircraft Structures in High-Speed Flight. Nr. 5, Mitt. Inst. Flugzeugstatik Leichtbau, Leeman (Zürich), c.1958.

4. Dixon, Sidney C.: Application of Transtability Concept to Flutter of Finite Panels and Experimental Results. NASA TN D-1948, 1963.

5. Bohon, Herman L.; and Anderson, Melvin S.: The Role of Boundary Conditions on Flutter of Orthotropic Panels. AIAA Symposium on Structural Dynamics and Aeroelasticity, Aug.-Sept. 1965, pp. 59-69.

6. Libove, Charles; and Batdorf, S. B.: A General Small-Deflection Theory for Flat Sandwich Plates. NACA Rept. 899, 1948. (Supersedes NACA TN 1526.)

7. Bohon, Herman L.; and Dixon, Sidney C.: Some Recent Developments in Flutter of Flat Panels. J. Aircraft, vol. 1, no. 5, Sept.-Oct. 1964, pp. 280-288.

8. Kantorovich, L. V.; and Krylov, V. I. (Curtis D. Benster, trans.): Approximate Methods of Higher Analysis. Interscience Publ., Inc., 1958, p. 304.

9. Movchan, A. A.: On the Stability of a Panel Moving in a Gas. NASA RE 11-21-58W, 1959.

10. Weeks, George E.; and Shideler, John L.: Effect of Edge Loadings on the Vibration of Rectangular Plates With Various Boundary Conditions. NASA TN D-2815, 1965.

11. Bolotin, V. V. (T. K. Lusher, trans.): Nonconservative Problems of the Theory of Elastic Stability. The Macmillan Co., 1963, p. 250.

TABLE I.- FLUTTER SOLUTIONS FOR FLAT RECTANGULAR PANELS WITH VARIOUS DEGREES OF ROTATIONAL EDGE RESTRAINT

$\bar{A}$	$q_x = 0$			$q_x = 2$			$q_x = 10$		
	λ_{cr}	$\bar{B}_{cr}$	α_{cr}	λ_{cr}	$\bar{B}_{cr}$	α_{cr}	λ_{cr}	$\bar{B}_{cr}$	α_{cr}
-300	92,230	8,584	21.96	92,240	8,594	21.91	92,300	8,606	21.91
-200	51,390	4,060	17.89	51,410	4,063	17.90	51,470	4,078	17.87
-100	19,410	1,200	12.68	19,430	1,202	12.70	19,500	1,212	12.71
-70	11,980	667.5	10.64	12,000	670.0	10.66	12,080	680.0	10.66
-50	7,720	395.0	9.082	7,747	397.5	9.099	7,825	407.5	9.085
-40	5,830	285.0	8.164	5,858	287.5	8.183	5,938	296.4	8.186
-30	4,119	190.5	7.177	4,149	193.5	7.179	4,231	202.0	7.182
-20	2,608	113.5	6.014	2,640	116.5	6.014	2,725	124.0	6.032
-10	1,330	53.50	4.582	1,364	56.50	4.574	1,452	63.00	4.616
-5	794.6	30.05	3.669	830.5	32.50	3.686	918.5	38.50	3.744
-4	697.1	25.75	3.467	733.3	28.25	3.482	821.4	34.25	3.540
-3	603.1	21.80	3.242	639.6	24.21	3.264	727.7	29.90	3.339
-2	512.6	18.00	3.004	549.5	20.40	3.027	637.5	25.80	3.122
-1	426.0	14.30	2.752	463.1	16.55	2.788	551.0	21.95	2.888
0	343.3	10.75	2.480	380.8	13.00	2.520	468.4	18.25	2.637
1	264.9	7.500	2.165	302.6	9.625	2.224	389.8	14.62	2.373
2	190.9	4.375	1.810	228.9	6.375	1.895	315.5	11.12	2.087
3	121.8	1.375	1.387	160.0	3.375	1.508	245.8	7.875	1.766
4	57.98	-1.412	.8262	96.21	.4500	1.049	180.9	4.700	1.415
5	0	-4	0	38.16	-2.250	.4702	121.2	1.625	1.024
6	51.27	-6.400	.7211	13.48	-4.800	.1659	67.18	-1.250	.5948
7	94.54	-8.625	1.047	57.70	-7.212	.6184	19.46	-4.045	.1716
8	127.5	-10.69	1.171	92.94	-9.500	.8490	21.21	-6.775	.1764
9	145.5	-12.75	1.163	116.6	-11.75	.9288	53.81	-9.500	.4099
10	137.3	-16.25	1.048	123.8	-14.62	.9031	76.92	-12.37	.5361
11	99.85	-22.50	.8293	108.6	-18.87	.7715	88.81	-15.50	.5717
12	51.01	-29.37	.4818	74.48	-25.00	.5506	87.75	-19.37	.5341
13	0	-36	0	32.25	-31.60	.2484	73.77	-24.25	.4344
14	49.67	-42.40	.4682	11.61	-38.12	.0891	50.01	-30.15	.2899
15	96.08	-48.55	.7857	53.91	-44.55	.3915	21.09	-36.60	.1204
16	137.7	-54.50	.9802	92.63	-50.86	.6185	9.167	-43.30	.0510
17	172.7	-60.39	1.093	126.1	-57.10	.7700	38.17	-50.15	.2050
18	199.0	-66.25	1.140	152.6	-63.49	.8594	64.04	-57.20	.3298
19	212.8	-72.60	1.132	169.8	-70.20	.8941	85.34	-64.45	.4201
20	208.2	-81.00	1.081	175.2	-77.75	.8803	100.8	-72.00	.4750
21	183.2	-92.60	.9919	166.3	-87.00	.8234	109.5	-80.20	.4973

TABLE I.- FLUTTER SOLUTIONS FOR FLAT RECTANGULAR PANELS WITH

VARIOUS DEGREES OF ROTATIONAL EDGE RESTRAINT — Concluded

$\overline{A}$	$q_X = 40$			$q_X = \infty$		
	λ_{cr}	$\overline{B}_{cr}$	α_{cr}	λ_{cr}	$\overline{B}_{cr}$	α_{cr}
-300	92,400	8,638	21.86	92,630	8,684	21.95
-200	51,590	4,100	17.89	51,790	4,142	17.89
-100	19,620	1,232	12.69	19,790	1,257	12.71
-70	12,200	695.0	10.69	12,350	717.5	10.67
-50	7,946	422.5	9.082	8,085	437.5	9.128
-40	6,058	310.0	8.190	6,189	323.7	8.197
-30	4,348	215.0	7.169	4,470	226.0	7.226
-20	2,839	134.5	6.054	2,949	144.0	6.097
-10	1,560	71.00	4.679	1,655	78.50	4.723
-5	1,022	45.50	3.828	1,107	51.50	3.894
-4	923.4	41.00	3.633	1,006	46.50	3.712
-3	828.2	36.50	3.435	908.6	41.69	3.521
-2	736.5	32.20	3.227	814.5	37.20	3.316
-1	648.3	27.90	3.013	723.8	32.49	3.115
0	563.8	23.75	2.788	636.6	28.25	2.891
1	483.0	20.02	2.536	553.0	24.00	2.660
2	406.3	16.25	2.276	473.3	19.75	2.420
3	333.9	12.50	2.002	397.6	15.75	2.160
4	265.8	9.000	1.700	326.1	12.00	1.877
5	202.4	5.625	1.374	258.9	8.250	1.578
6	144.1	2.250	1.029	196.5	4.750	1.253
7	91.17	-.9000	.6670	138.9	1.250	.9172
8	44.08	-4.062	.3209	86.74	-2.217	.5804
9	3.373	-7.170	.0236	40.27	-5.614	.2654
10	30.27	-10.30	.1995	0	-9	0
11	56.07	-13.60	.3453	33.48	-12.50	.2005
12	73.14	-17.00	.4203	59.51	-16.00	.3348
13	80.73	-21.00	.4384	77.40	-19.85	.4102
14	78.58	-25.69	.4082	86.54	-24.10	.4347
15	67.60	-31.20	.3398	86.74	-29.00	.4169
16	49.96	-37.45	.2447	78.60	-34.70	.3651
17	28.40	-44.30	.1359	63.69	-41.20	.2882
18	5.411	-51.56	.0253	44.20	-48.32	.1954
19	17.04	-59.16	.0774	22.34	-55.97	.0966
20	37.48	-67.05	.1651	0	-64	0
21	54.80	-75.25	.2339	21.35	-72.36	.0878
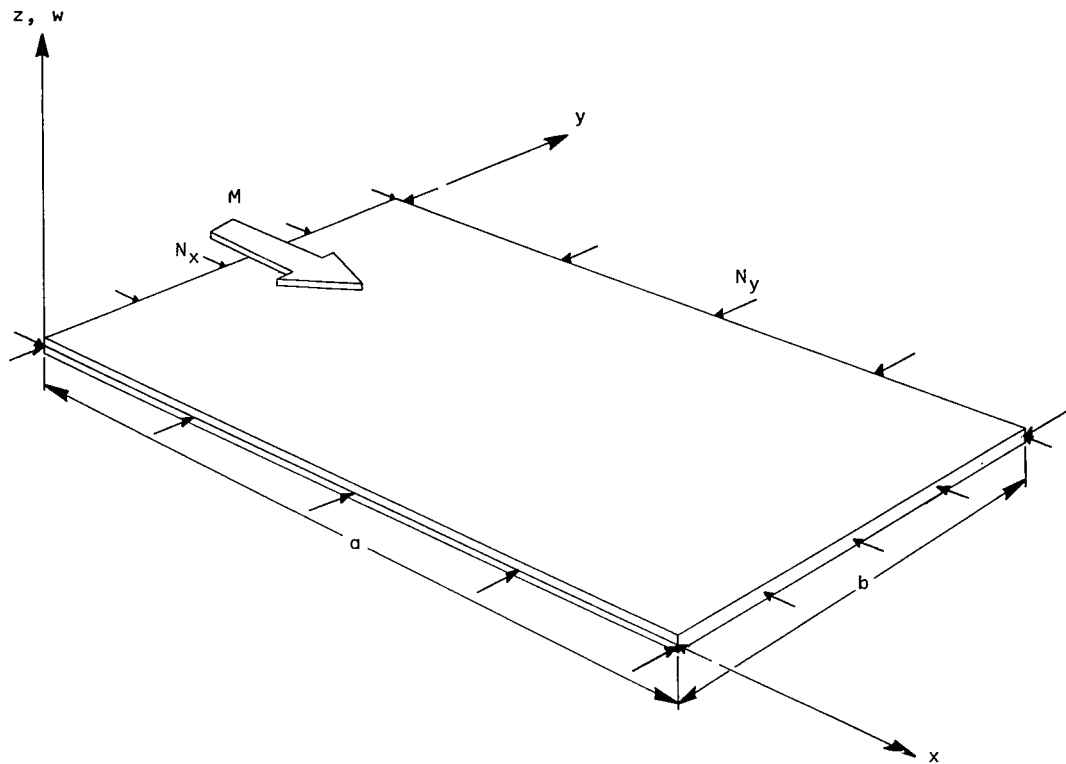
Figure 1.- Panel geometry, coordinate system, and flow direction.
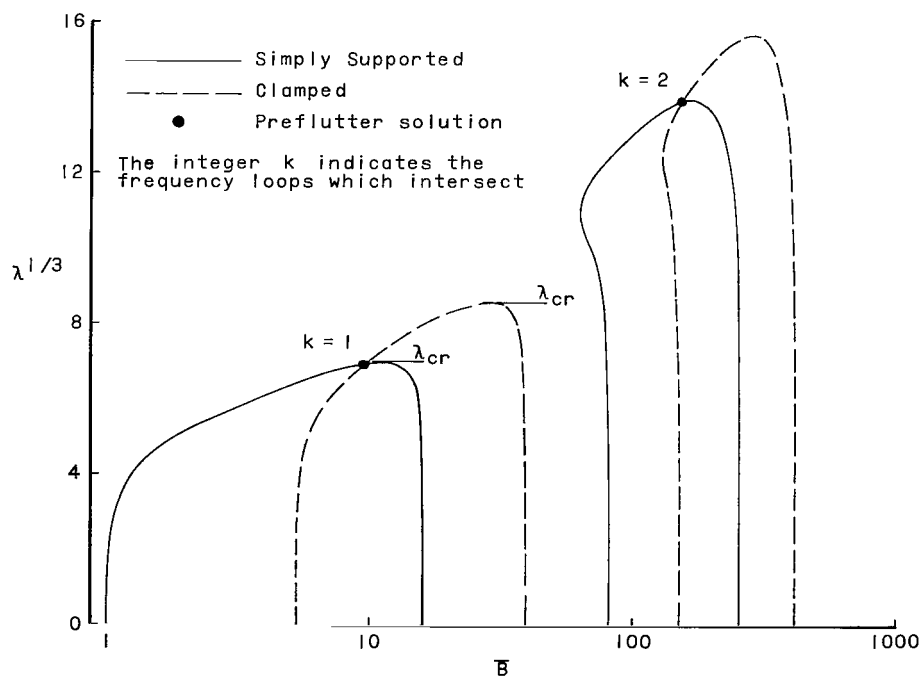
Figure 2.- First two frequency loops for clamped and simply supported panels. $\overline{A} = 0.$
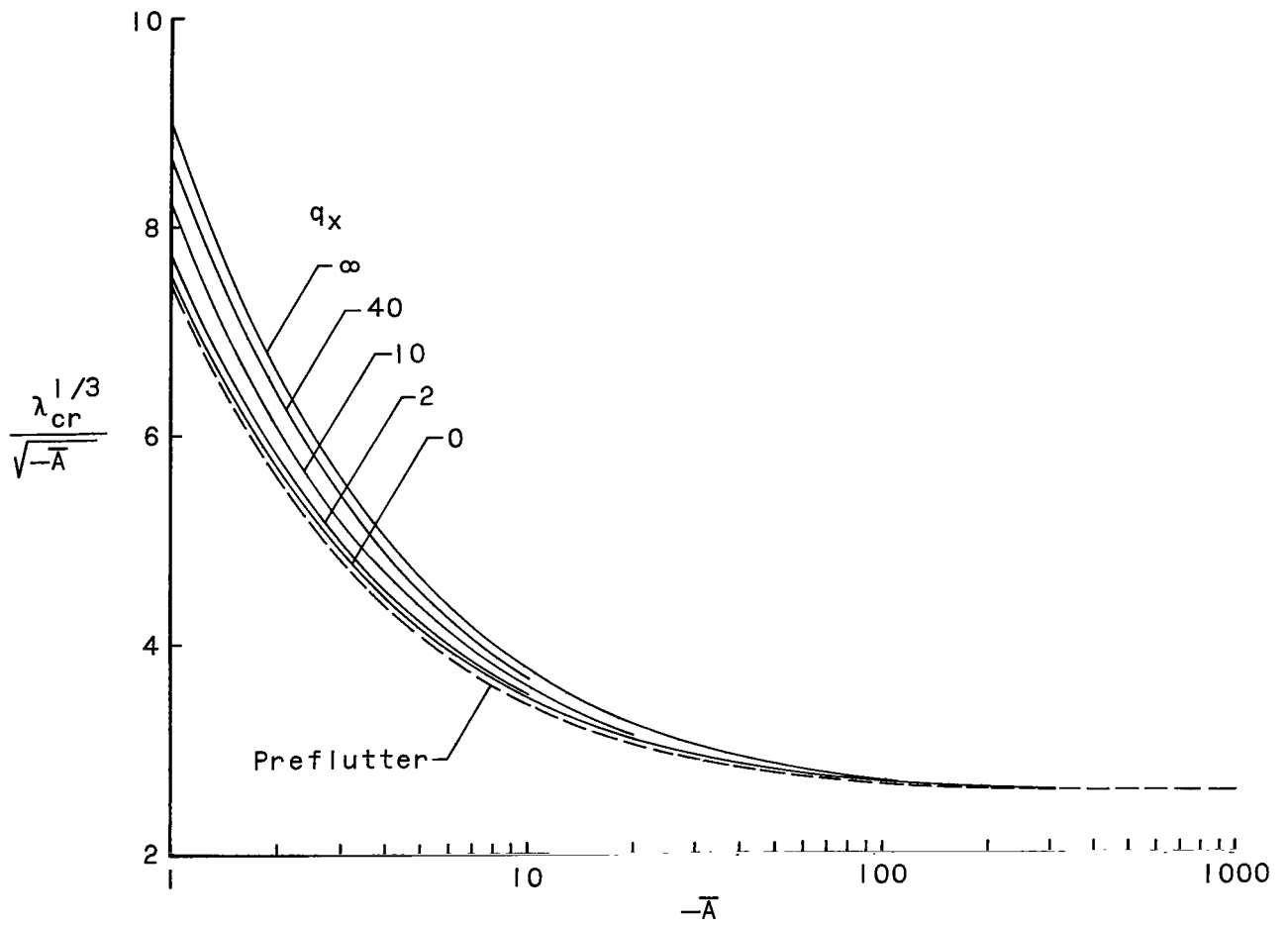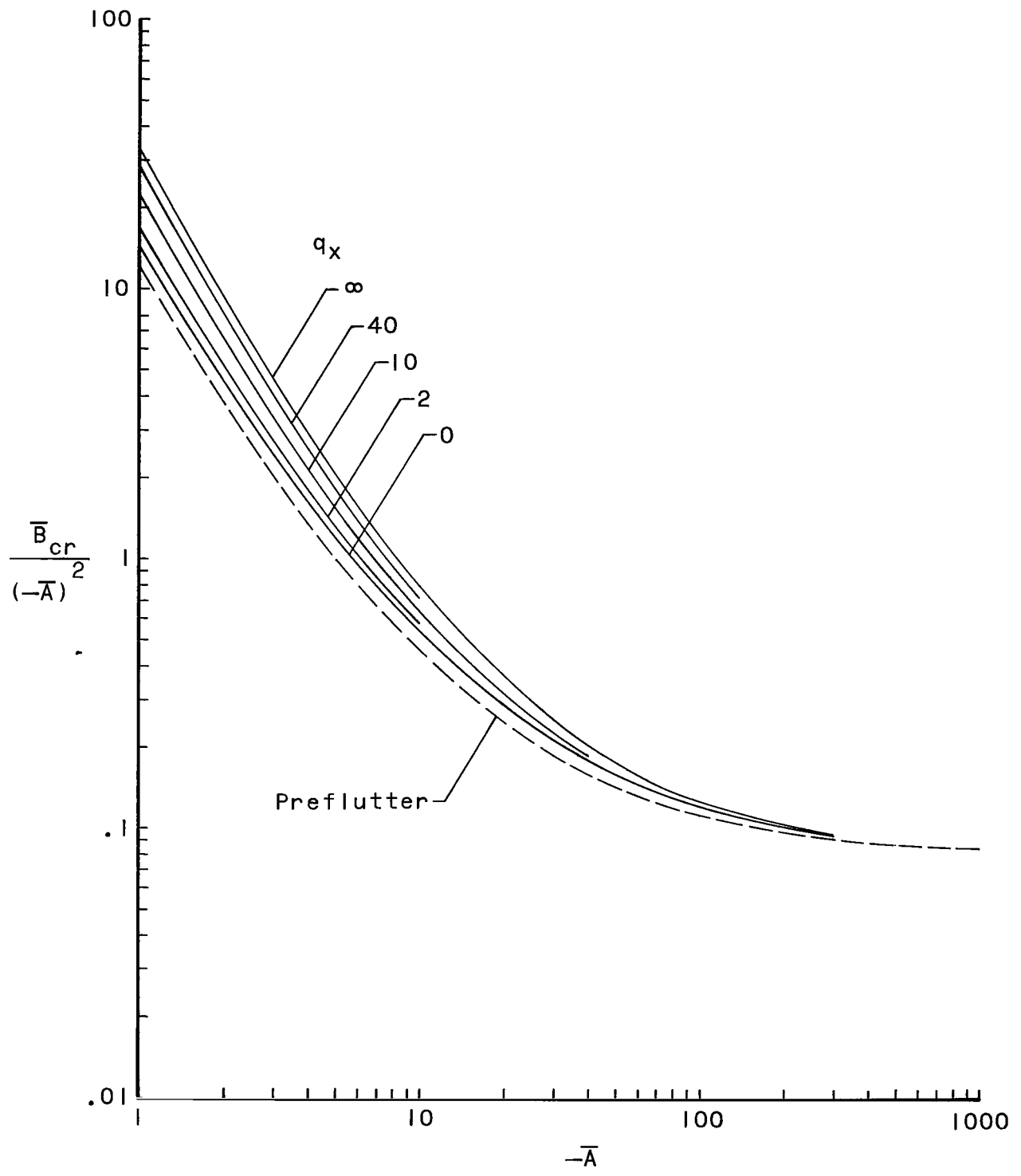
Figure 3.- Variation of λ_{cr} with negative $\overline{A}$ for panels with various degrees of rotational restraint on leading and trailing edges.
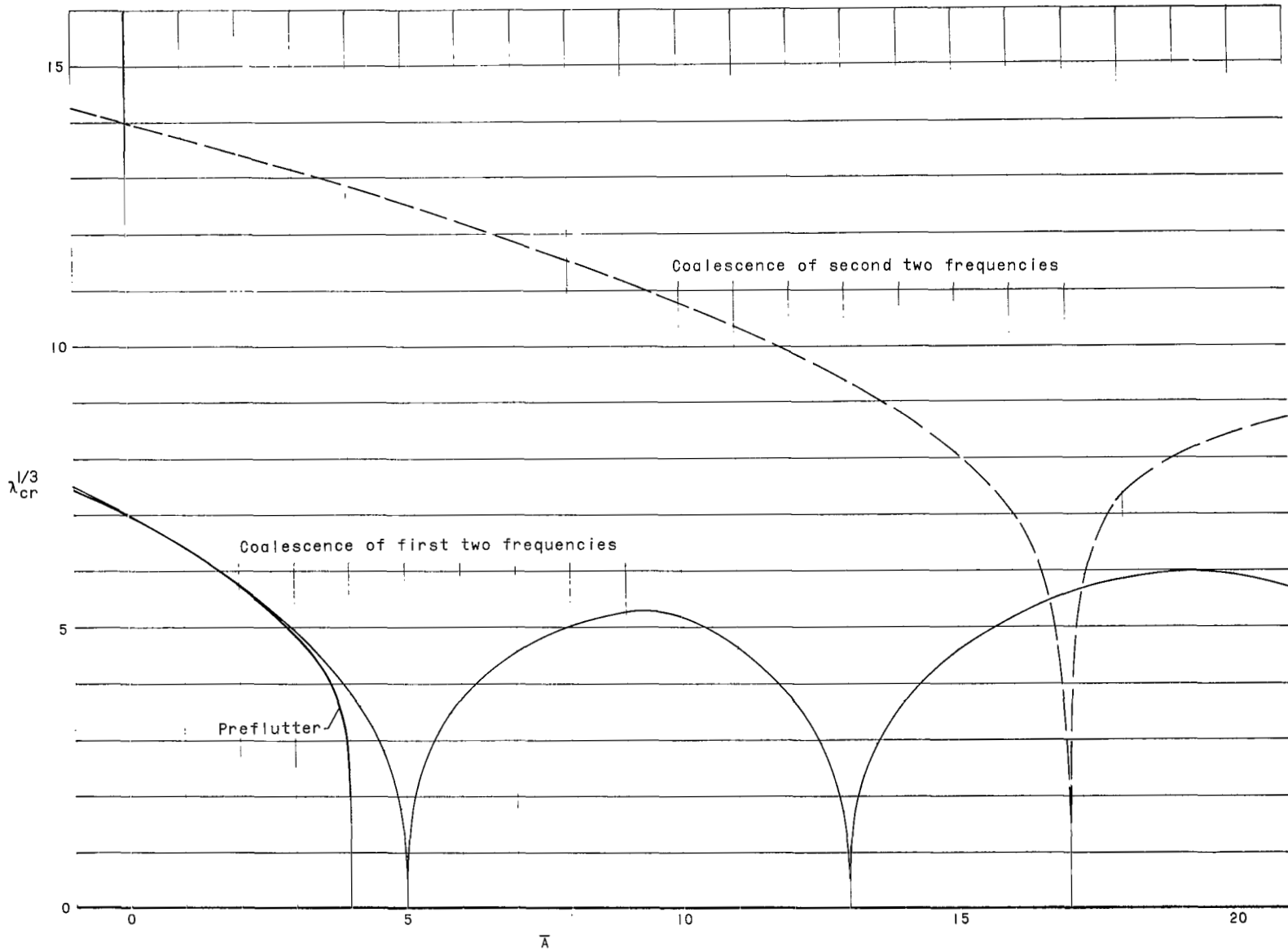
Figure 4.- Variation of $\overline{B}_{cr}$ with negative $\overline{A}$ for panels with various degrees of rotational restraint on leading and trailing edges.

Figure 5.- Variation of λ_{cr} with positive $\overline{A}$ for panel with simply supported leading and trailing edges. $q_x = 0$.
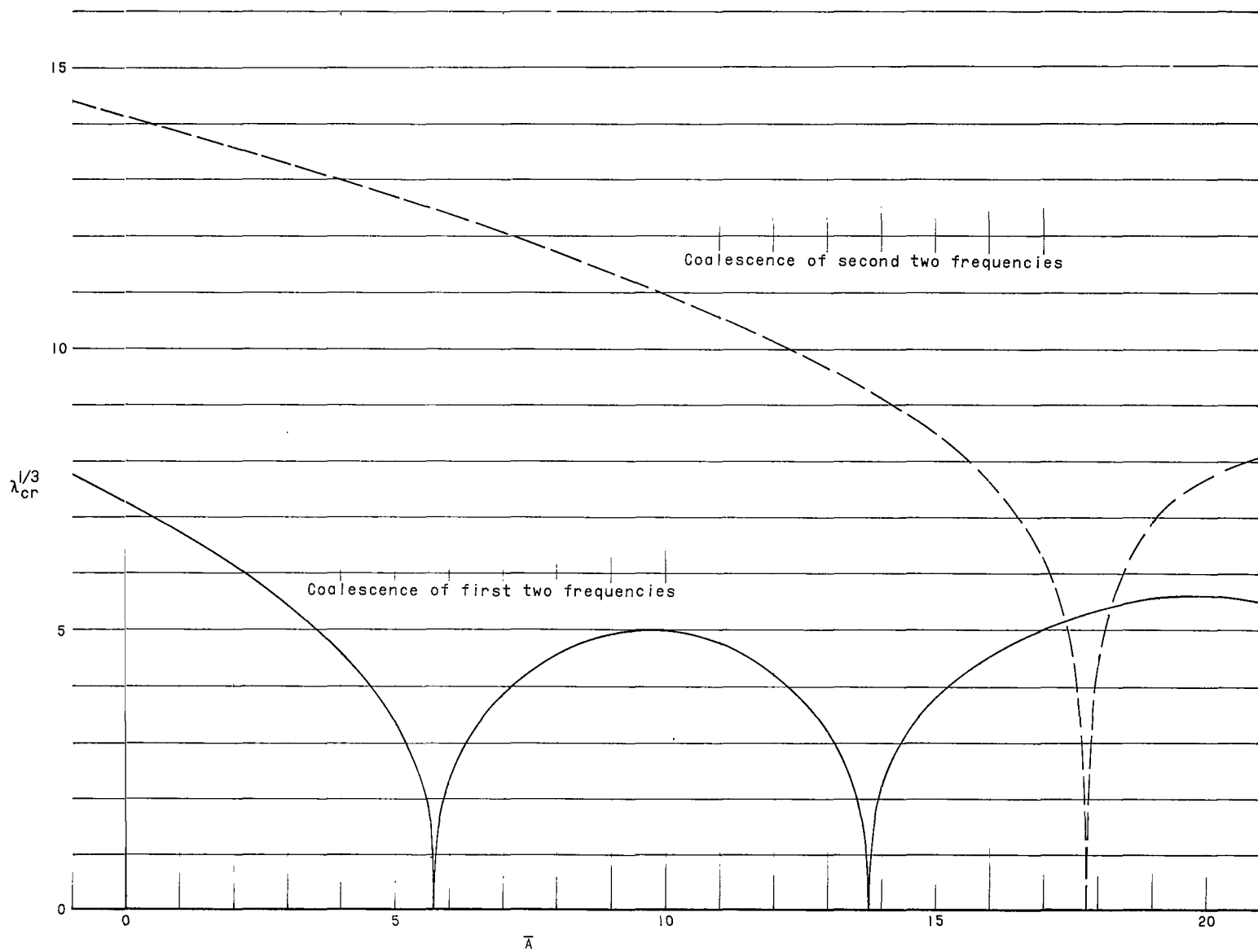
Figure 6.- Variation of λ_{cr} with positive $\overline{A}$ for panel with rotational restraints at leading and trailing edges. $q_x = 2$.
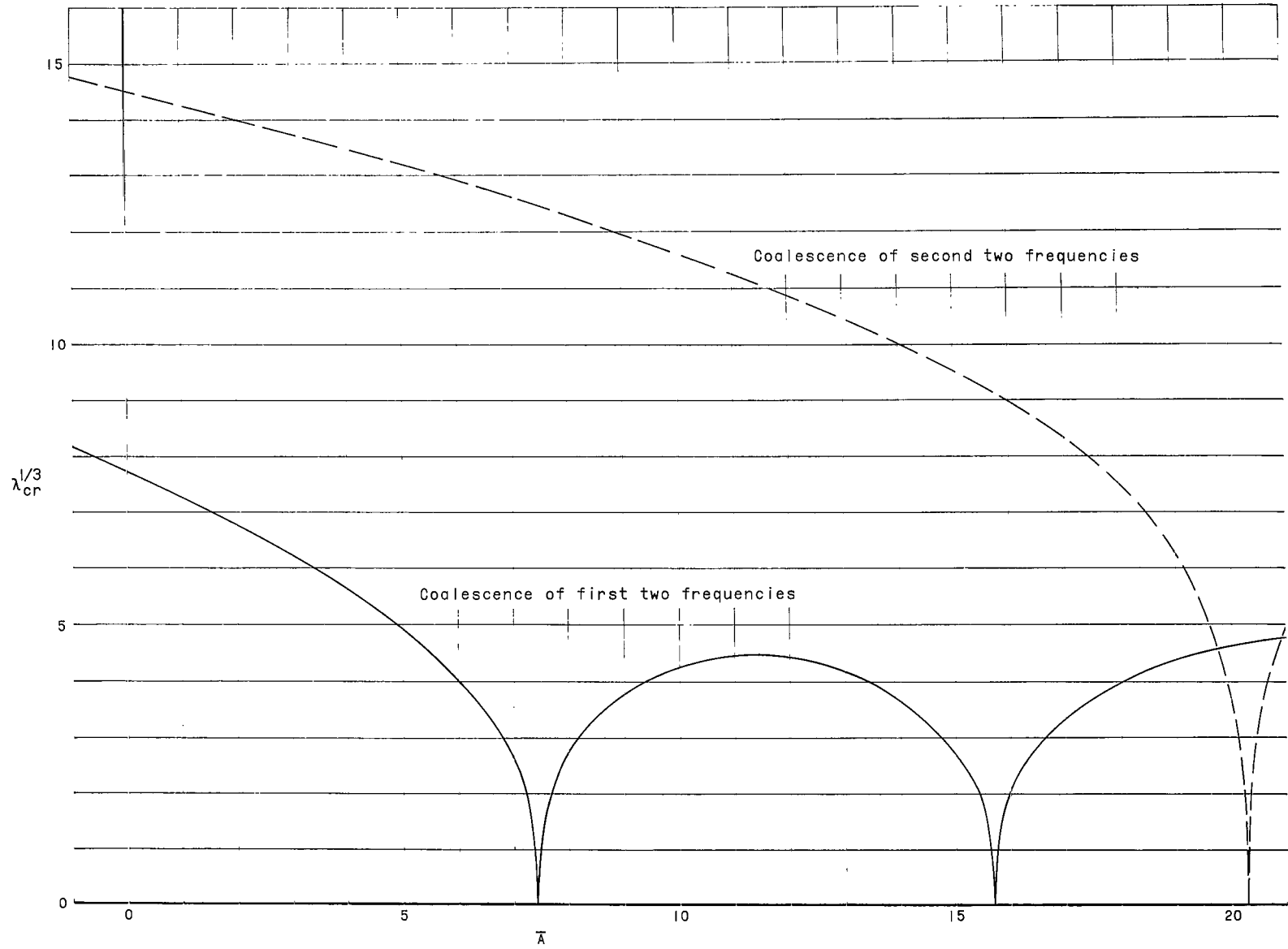
Figure 7.- Variation of λ_{cr} with positive $\overline{A}$ for panel with rotational restraints at leading and trailing edges. $q_x = 10$.
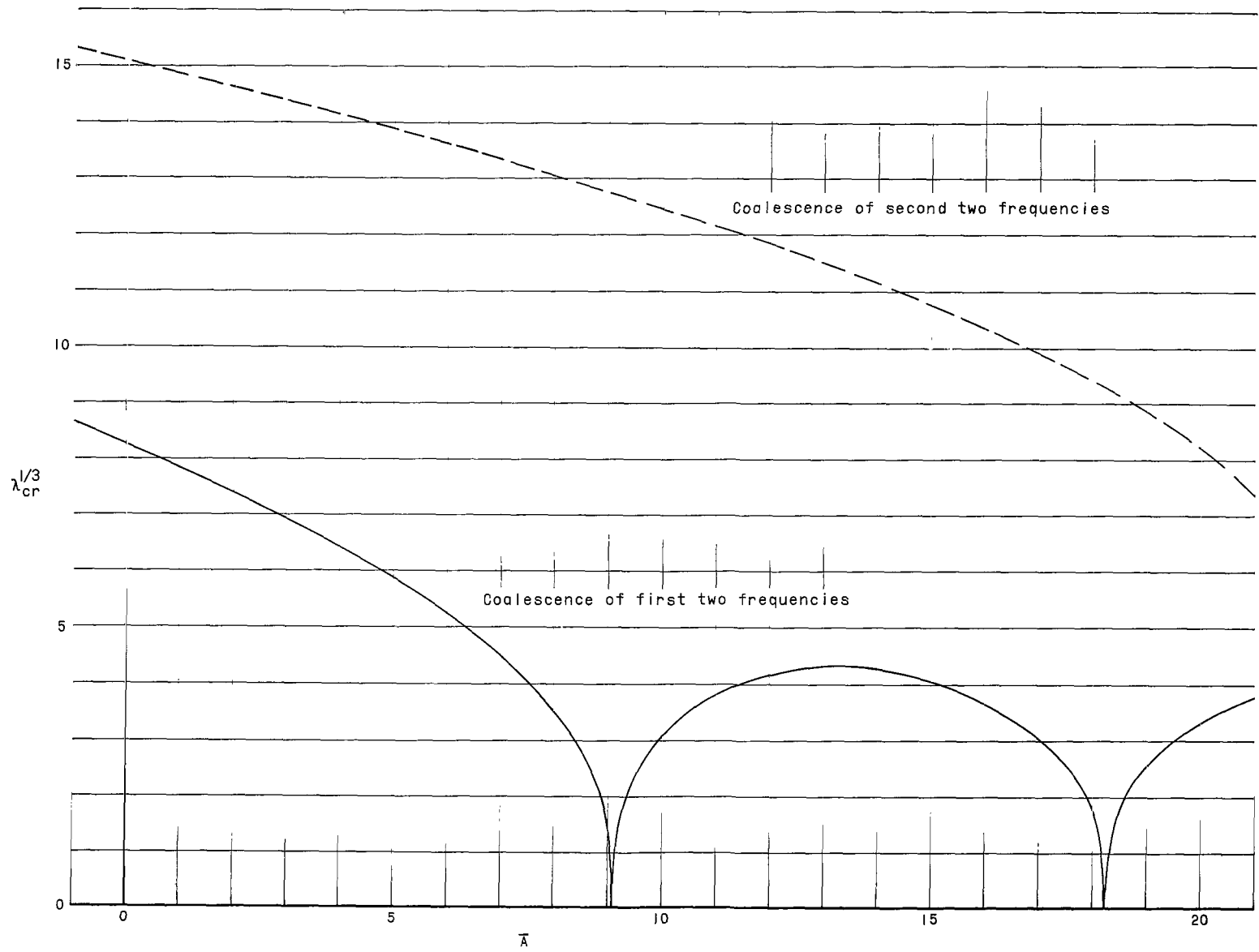
Figure 8.- Variation of λ_{cr} with positive $\overline{A}$ for panel with rotational restraints at leading and trailing edges. $q_x = 40$.
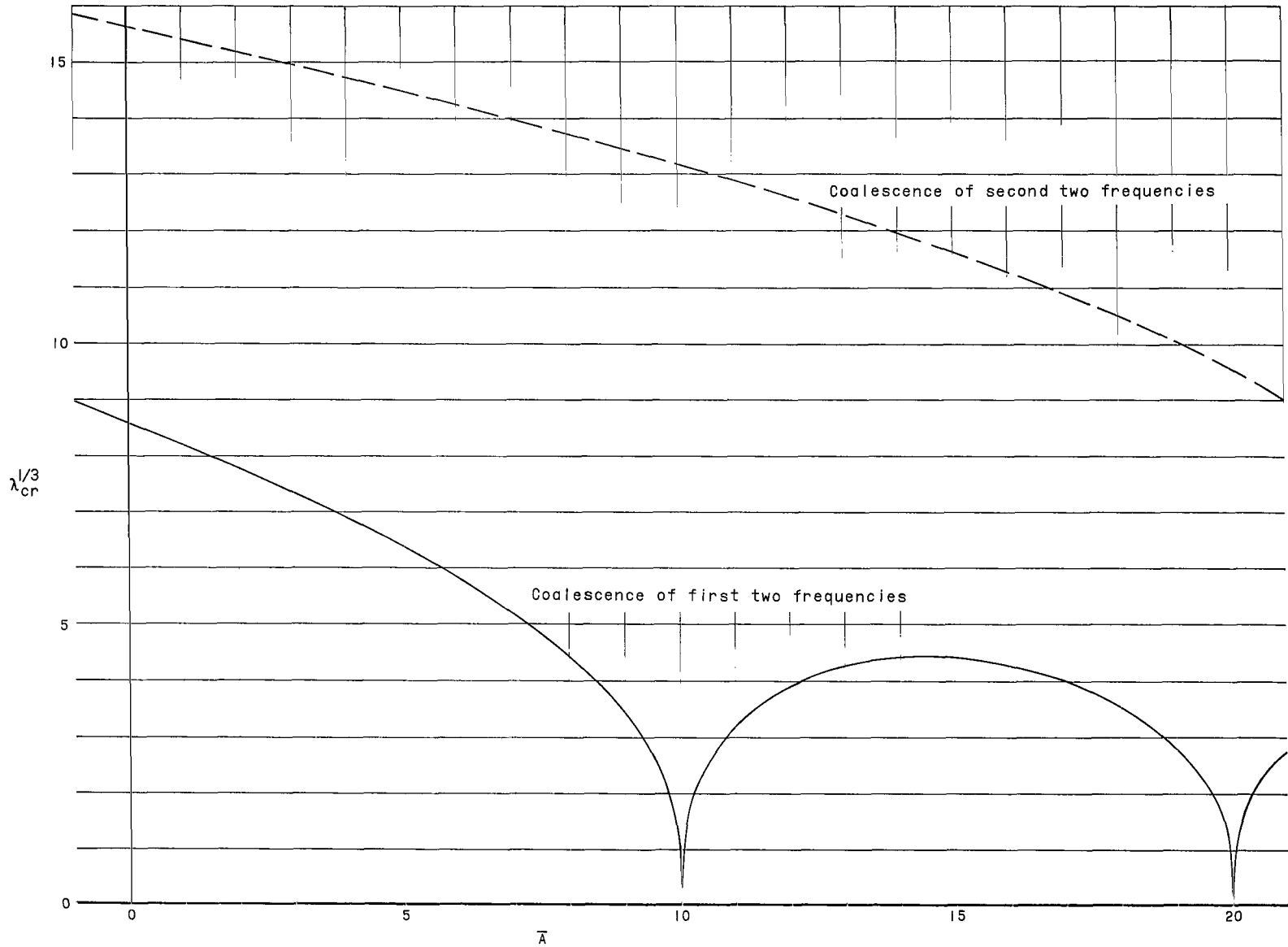
Figure 9.- Variation of λ_{cr} with positive $\overline{A}$ for panel with clamped leading and trailing edges. $q_x = \infty$.
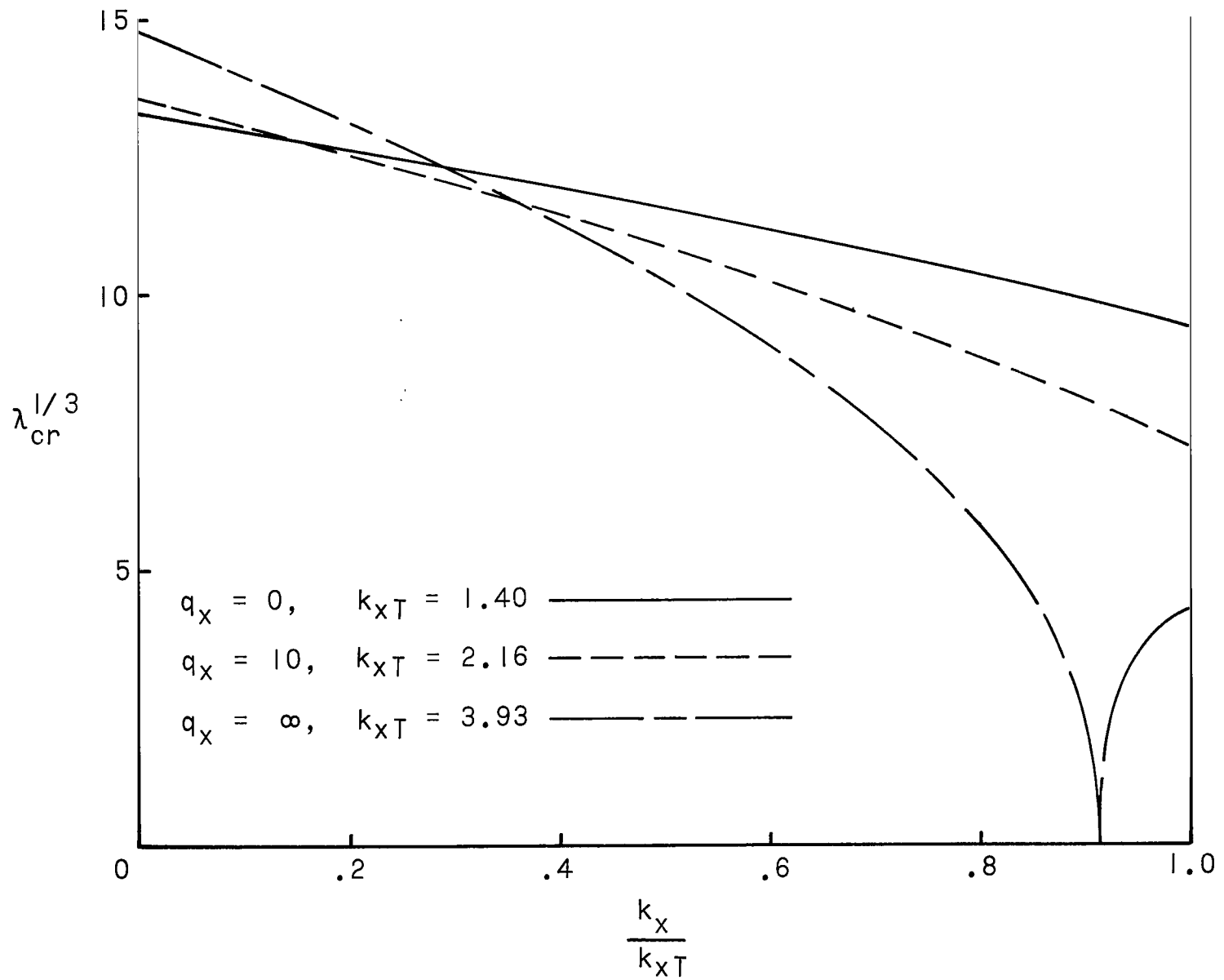
Figure 10.- Variation in λ_{cr} with stress ratio for different boundary conditions. $a/b = 3$; $N_y/N_x = 1$; $\theta_y/\theta_x = 1$; $D_1 = D_{12} = D_2$.
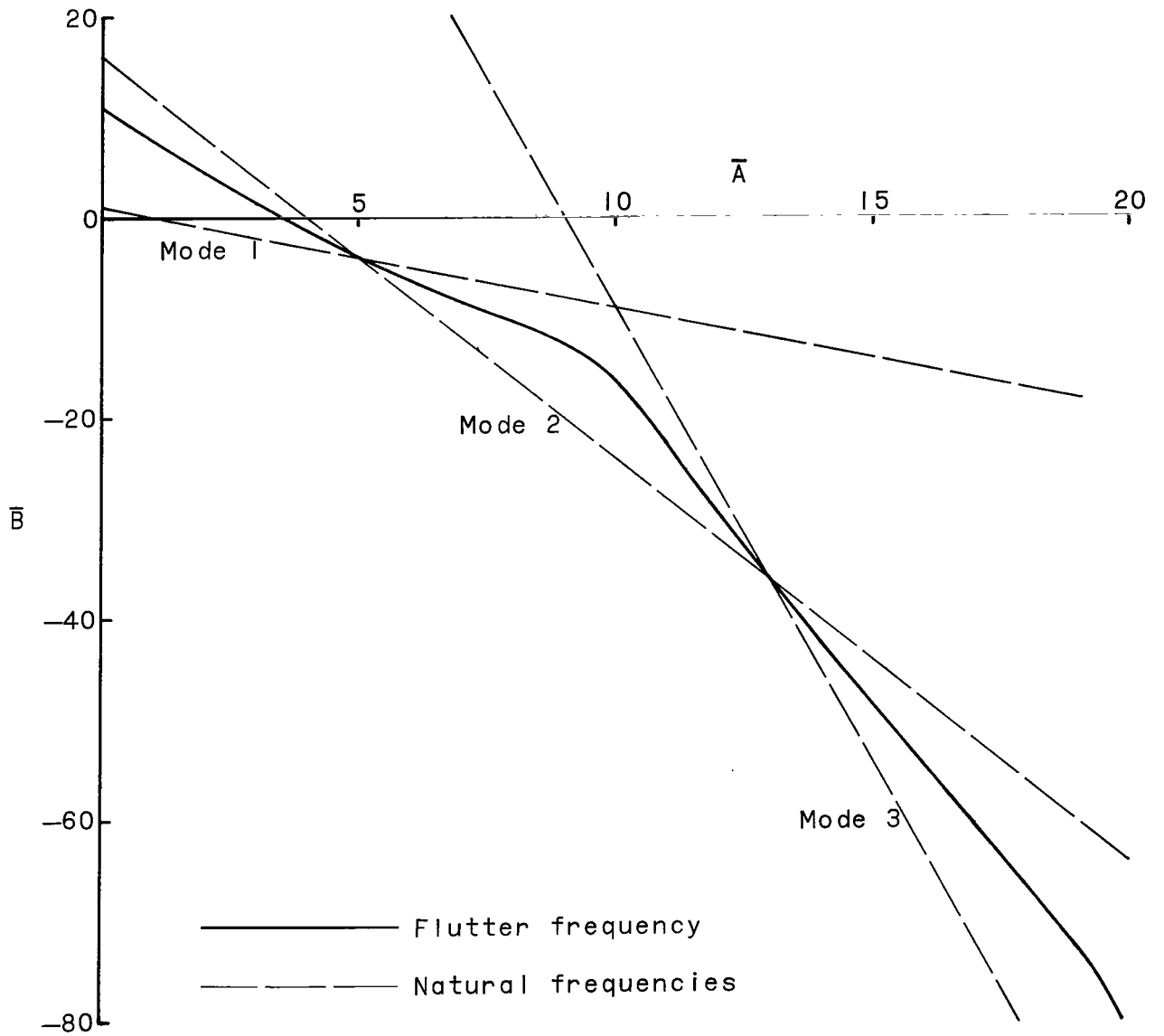
(a) Simply supported leading and trailing edges.

Figure 11.- Variation of $\bar{B}$ with positive $\bar{A}$.
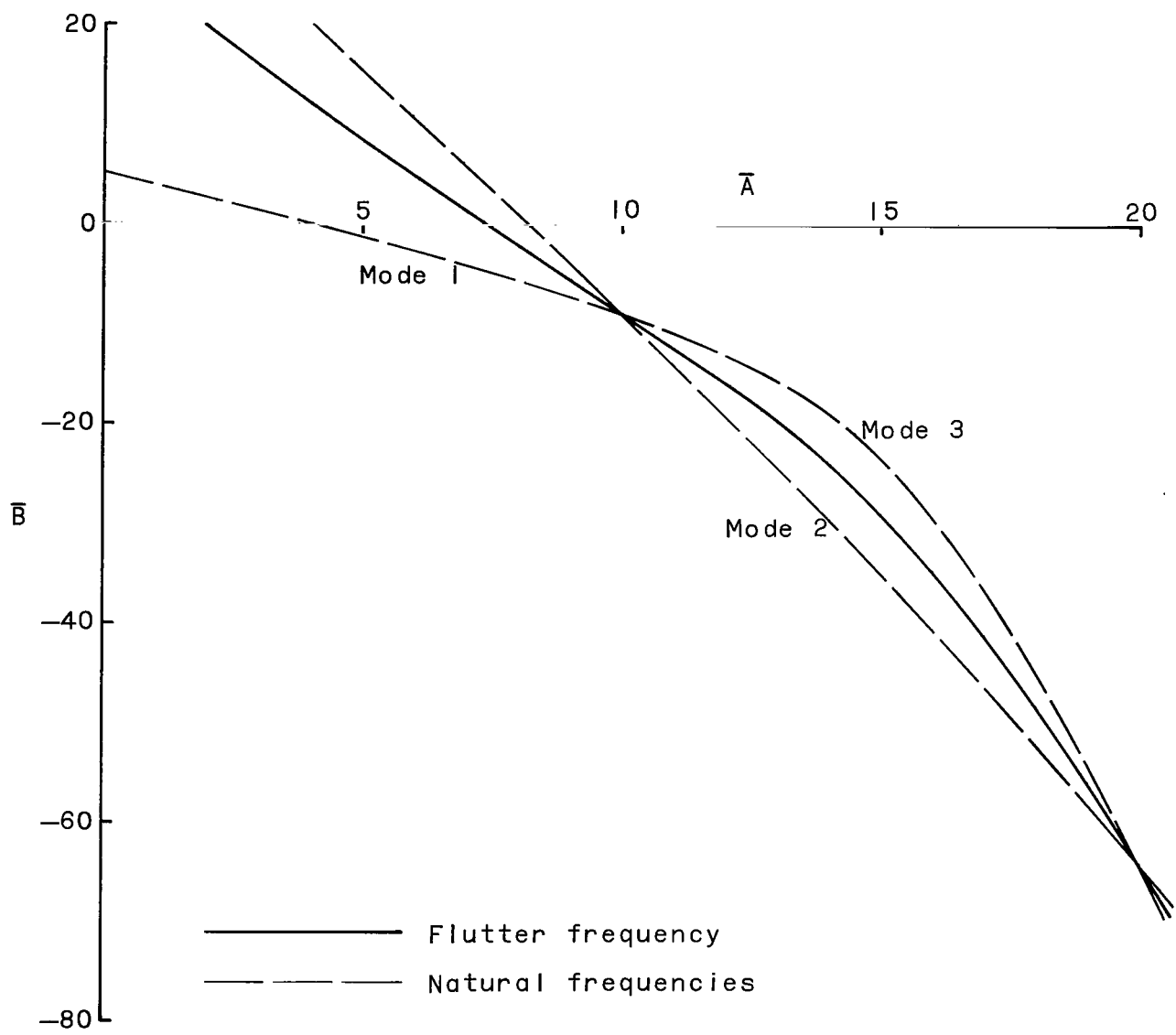
(b) Clamped leading and trailing edges.

Figure 11.- Concluded.
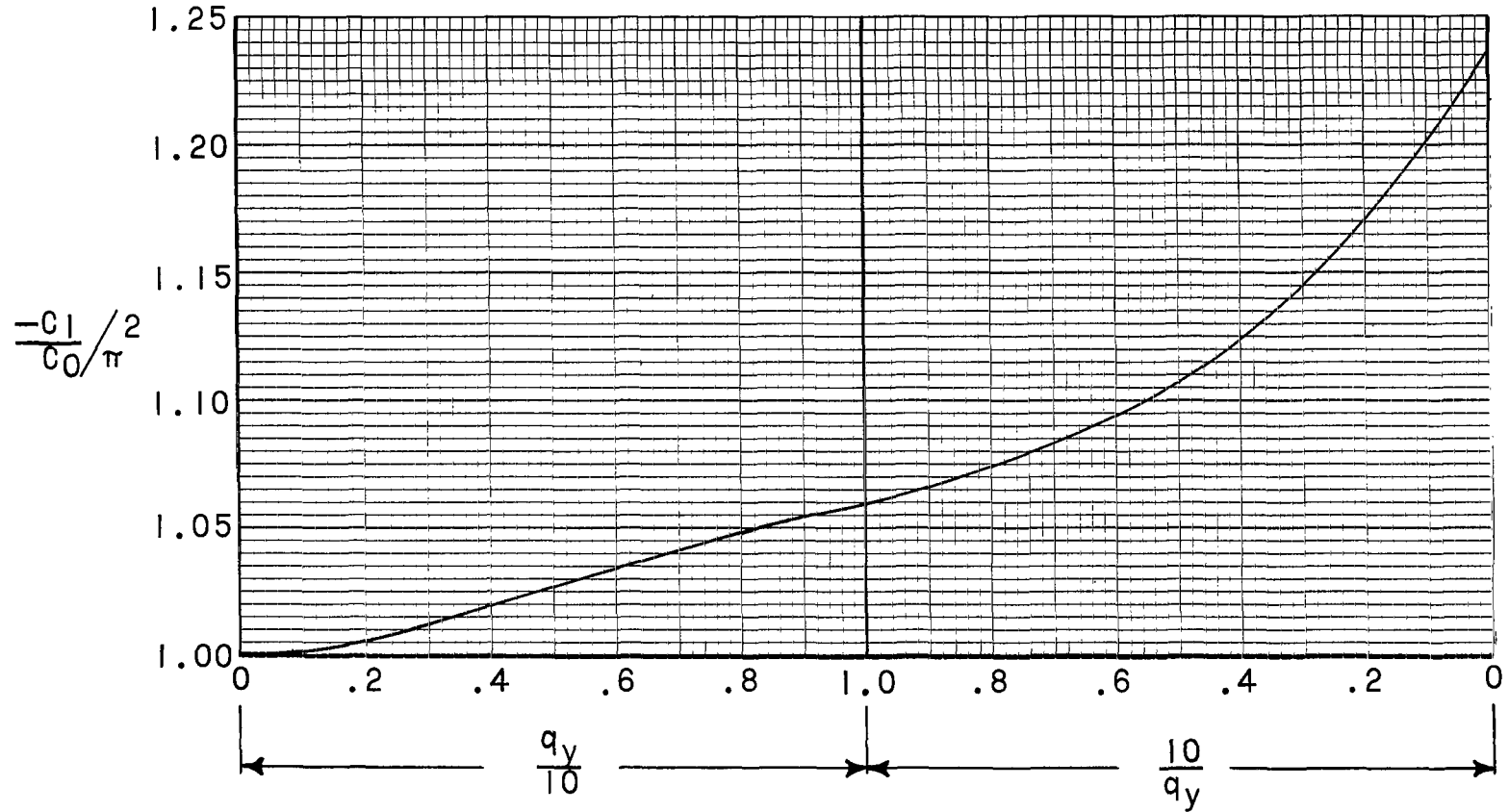
Figure 12.- Variation of C_1/C_0 with rotational restraint coefficient q_y for first mode in y-direction.
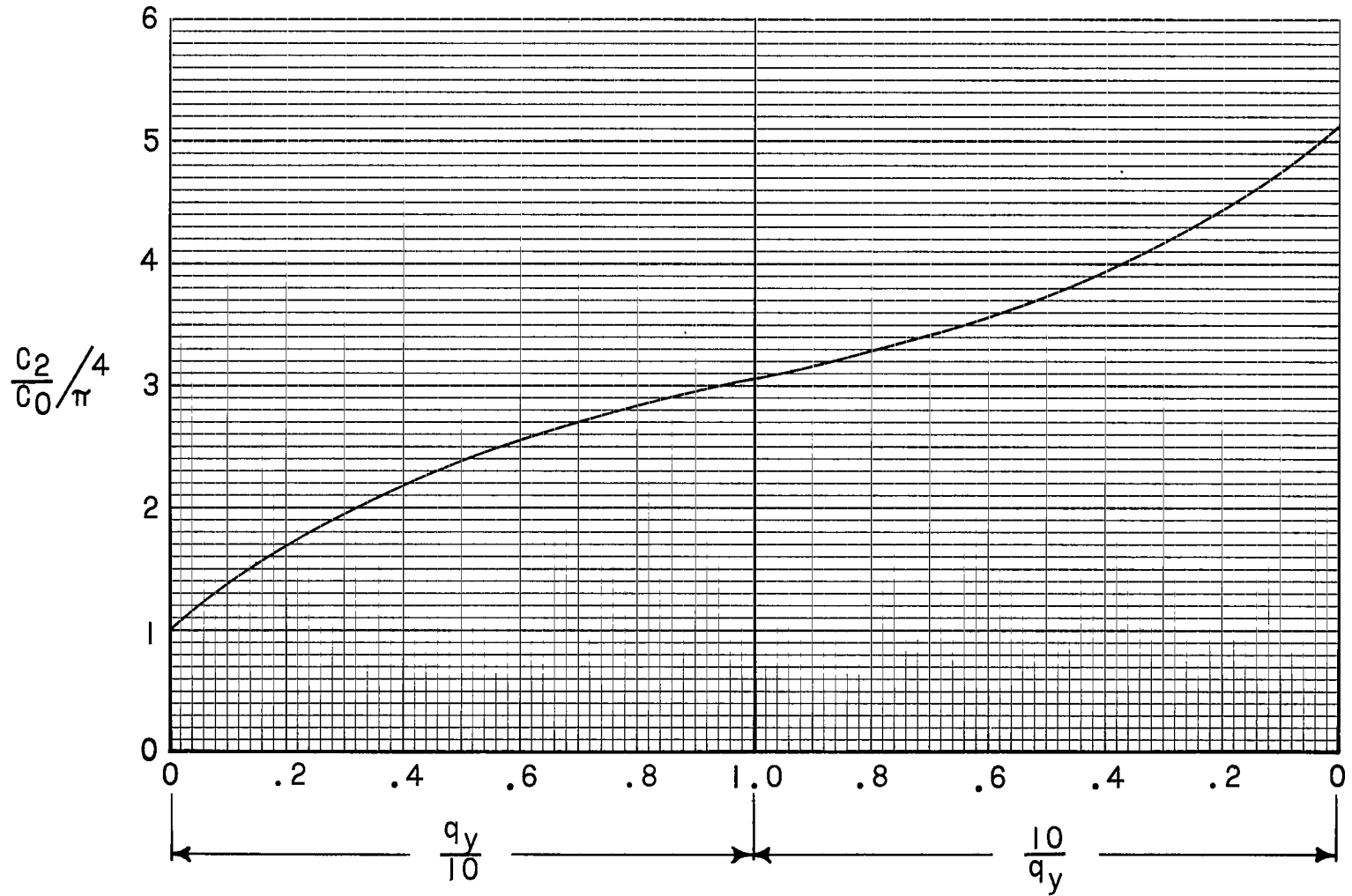
Figure 13.- Variation of C_2/C_0 with rotational restraint coefficient q_y for first mode in y-direction.
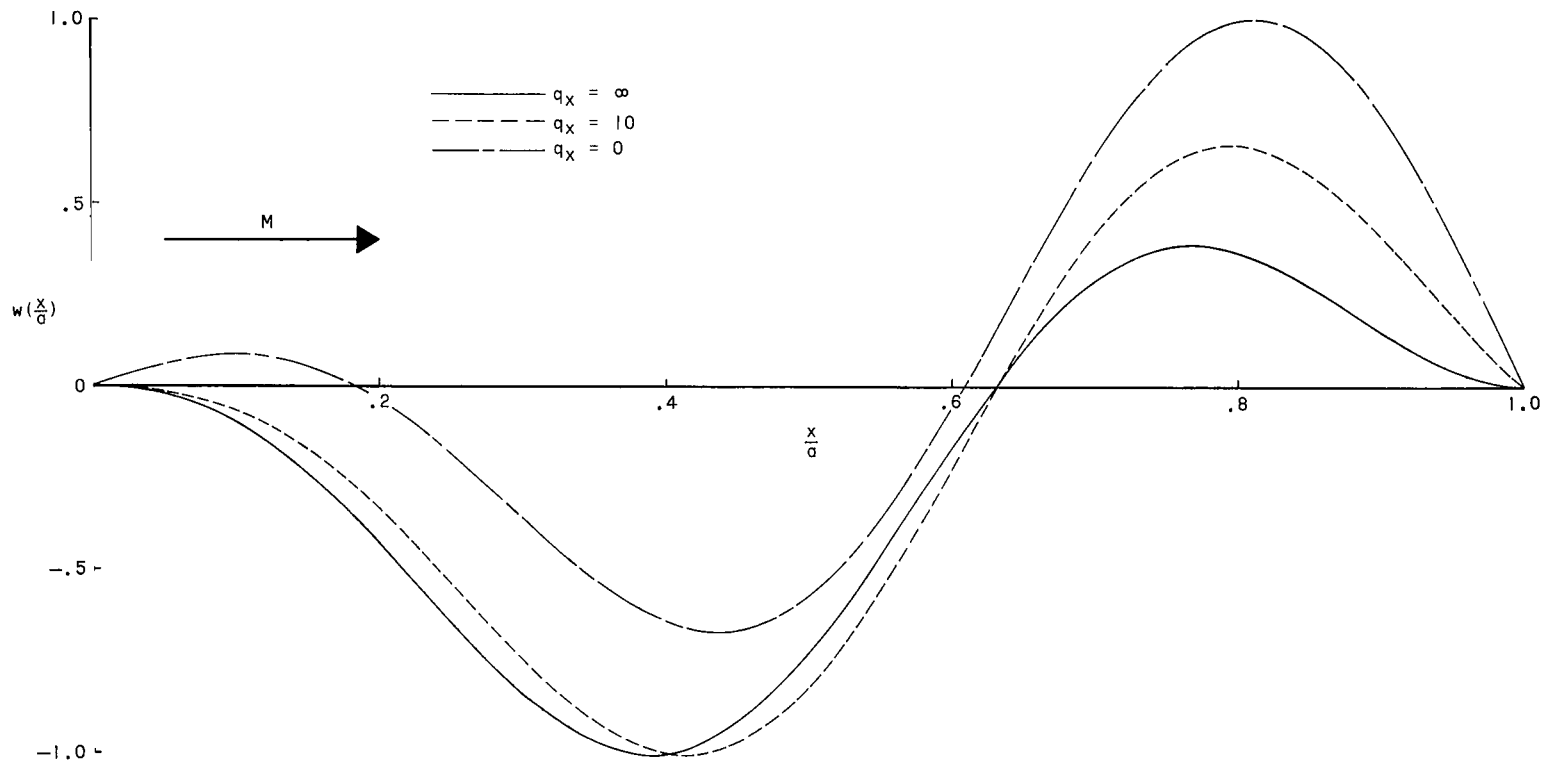
Figure 14.- Normalized mode shapes at flutter showing effect of different degrees of rotational edge restraint. $\overline{A} = 12$.

NASA SCIENTIFIC AND TECHNICAL PUBLICATIONS

TECHNICAL REPORTS: Scientific and technical information considered important, complete, and a lasting contribution to existing knowledge.

TECHNICAL NOTES: Information less broad in scope but nevertheless of importance as a contribution to existing knowledge.

TECHNICAL MEMORANDUMS: Information receiving limited distribution because of preliminary data, security classification, or other reasons.

CONTRACTOR REPORTS: Technical information generated in connection with a NASA contract or grant and released under NASA auspices.

TECHNICAL TRANSLATIONS: Information published in a foreign language considered to merit NASA distribution in English.

TECHNICAL REPRINTS: Information derived from NASA activities and initially published in the form of journal articles.

SPECIAL PUBLICATIONS: Information derived from or of value to NASA activities but not necessarily reporting the results of individual NASA-programmed scientific efforts. Publications include conference proceedings, monographs, data compilations, handbooks, sourcebooks, and special bibliographies.